International Journal of Engineering, Mathematical and Physical Sciences
ISSN: 2517-9934
Vol:10, No:2, 2016

# Combined Effect of Moving and Open Boundary Conditions in the Simulation of Inland Inundation Due to Far Field Tsunami

M. Ashaque Meah, Md. Fazlul Karim, M. Shah Noor, Nazmun Nahar Papri, M. Khalid Hossen, M. Ismoen

***Abstract*—**Tsunami and inundation modelling due to far field tsunami propagation in a limited area is a very challenging numerical task because it involves many aspects such as the formation of various types of waves and the irregularities of coastal boundaries. To compute the effect of far field tsunami and extent of inland inundation due to far field tsunami along the coastal belts of west coast of Malaysia and Southern Thailand, a formulated boundary condition and a moving boundary condition are simultaneously used. In this study, a boundary fitted curvilinear grid system is used in order to incorporate the coastal and island boundaries accurately as the boundaries of the model domain are curvilinear in nature and the bending is high. The tsunami response of the event 26 December 2004 along the west open boundary of the model domain is computed to simulate the effect of far field tsunami. Based on the data of the tsunami source at the west open boundary of the model domain, a boundary condition is formulated and applied to simulate the tsunami response along the coastal and island boundaries. During the simulation process, a moving boundary condition is initiated instead of fixed vertical seaside wall. The extent of inland inundation and tsunami propagation pattern are computed. Some comparisons are carried out to test the validation of the simultaneous use of the two boundary conditions. All simulations show excellent agreement with the data of observation.

***Keywords*—**Open boundary condition, moving boundary condition, boundary-fitted curvilinear grids, far field tsunami, Shallow Water Equations, tsunami source, Indonesian tsunami of 2004.

## I. Introduction

AS because of the long wave characteristics of tsunami it causes serious damage not only the countries located near the earthquake source but also the countries far away from the source zone. So construction of realistic and reliable tsunami inundation mapping and tsunami height measurement along the coastal areas of concern are necessary. The three phases of a tsunami: generation, propagation and run-up are equally important for the accurate simulation of water levels in the coastal area for a near field or a local tsunami. But for distant tsunami the propagation and inundation phase become more important, since the time required for propagation is much longer than those for other phases [1]. However, the effect of a tsunami source along a particular coastal area far away from the region of interest may be significant if the waves move through deep Ocean. Since the response of the 2004 Indonesian tsunami reached every distant corner of the globe, it is necessary to estimate the response along a particular region due to a source located far away from that region. This may be done through a global model that contains both the source and the region of interest. Numerical models are good enough to simulate tsunami. After knowing the tsunami source, the tsunami propagation and coastal behavior can be modeled by computer simulation [2]–[8]. Kowalik et al. [6] developed a global model to simulate 2004 Indonesian tsunami. But a global model is not suitable for real time tsunami simulation, so regional model should be developed [5].

Boundary fitted curvilinear grid technique is used when the coastline is curvilinear in nature and the bending is high. It makes the equations and boundary conditions simple and better represents the complex geometry with a relatively less number of grid points. The boundary fitted grid system improves the finite difference schemes. The gridline of the numerical scheme is curvilinear and non-orthogonal in the boundary fitted grid system.

During the simulation of tsunami inland inundation, many researchers used moving boundary instead of fixed vertical seaside wall to properly represent the dynamics of the intrusion process [9]-[12]. Moving boundaries are associated with time dependent problems and the position of the boundary has to be determined as a function of time and space. The term moving boundary means the boundary at the edge of a water mass which is in motion with horizontally two–dimensional characteristics. Several types of moving boundary conditions have been proposed and used in the simulation of wave –front flooding on dry land [9]. All of them are based on the idea of so-called weir model in which a threshold depth is introduced to judge whether the water in the computational cell is moving or stopped.

In hydrodynamics computations problem arises when the theoretical model applies to an infinite or semi-infinite region. In this case, where the original domain of the problem under investigation is infinite or very large, open boundaries may be used. Open boundary is the idea of imaginary fixed boundary at which the outgoing wave from the domain is perfectly

M. A. Meah, M. S. Noor is with the Shahjalal University of Science and Technology (e-mail: mam-mat@sust.edu, imsnoor@yahoo.com)
M.F. Karim is with the Institut Teknologi Brunei, Brunei (phone: +673 7157167; e-mail: mdfazlulkk@yahoo.com, fazlul.karim@itb.edu.bn).
N. N. Papri is with the Leading University, Sylhet, Bangladesh (e-mail: npapri21@gmail.com)
M. K. Hossen is with the Sylhet Agriculture University, Bangladesh (e-mail: khalid@sau.ac.bd)
M. Ismoen is with the Institut Teknologi Brunei, Brunei (e-mail: muhaimin_ismoen@itb.edu.bn).

reflected to estimate the amplitude of the outgoing component. The main purpose of using the open boundaries is to allow waves and disturbances originating within the model domain to leave the domain without affecting the interior solution.

Karim et al. [12] developed a numerical model for estimating the extent of inundation along the coastal belt of Peninsular Malaysia and Thailand due to long waves associated with the 2004 Indonesian tsunami. Meah et al. [13] simulated the effect of far field tsunami along the coastal belt of Phuket and Penang Island through an open boundary condition in a boundary fitted curvilinear grid system. Since the Indonesian tsunami of 2004 is a global tsunami and it reaches every distant corner of the glove, so it is necessary to investigate the extent of inland inundation in various coastal locations which are far away from the tsunami source.

In this paper, we simulate the extent of inland inundation due to far field tsunami in a limited area model domain along the coastal belt of western coast of Peninsular Malaysia and southern Thailand. For this purpose, two models have been used. The source model (a boundary fitted curvilinear grid model) is used to compute the response of the source of Indonesian tsunami 2004 along the western open boundary of the model domain. Using the technique of [7] and based on the data computed from the source model, an appropriate boundary condition is formulated along the western open boundary of the model and at the same time the tsunami source near Sumatra is removed. This formulated boundary condition including with the moving boundary condition are then applied in the absence of the tsunami source in the model domain to simulate the extent of inland inundation as well as the tsunami run up along the coastal belts. Propagation history of 2004 event is also carried out to show the effect of moving boundary condition in the simulation process. Similar to [7] the moving boundary condition is used instead of fixed vertical sea side wall in the boundary fitted curvilinear grid system. Tsunami run up in various coastal locations and extent of inundation for different slope of the sea beach has been investigated and the simulated results have been found quite reasonable agreement with the data collected by the authors and data available in the websites.

## II. Numerical Model

The nonlinear shallow water equations are used here to model the 2004 Indonesian tsunami. Consider a rectangular Cartesian co-ordinate system in which the origin $O$ is in the undisturbed mean sea level (MSL), $x$- axis is directed towards west and $y$-axis is directed north on the MSL, whereas $z$-axis is directed vertically upwards. Let, the displaced position of the sea-surface is given by $z = \zeta(x, y, t)$ and the position of the sea-floor is given by $z = -h(x, y)$. So that depth of the fluid layer is $(\zeta + \eta)$.

Following [12], the vertically integrated shallow water equations in flux forms are:

$$\frac{\partial \zeta}{\partial t} + \frac{\partial \tilde{u}}{\partial x} + \frac{\partial \tilde{v}}{\partial y} = 0 \tag{1}$$

$$\frac{\partial \tilde{u}}{\partial t} + \frac{\partial (u\tilde{u})}{\partial x} + \frac{\partial (v\tilde{u})}{\partial y} - f\tilde{v} = -g(\zeta + h)\frac{\partial \zeta}{\partial x} - \frac{C_f \tilde{u}\left(u^2 + v^2\right)^{1/2}}{\zeta + h} \tag{2}$$

$$\frac{\partial \tilde{v}}{\partial t} + \frac{\partial (u\tilde{v})}{\partial x} + \frac{\partial (v\tilde{v})}{\partial y} + f\tilde{u} = -g(\zeta + h)\frac{\partial \zeta}{\partial y} - \frac{C_f \tilde{v}\left(u^2 + v^2\right)^{1/2}}{\zeta + h} \tag{3}$$

where, $(\tilde{u}, \tilde{v}) = (\zeta + h)(u, v)$ and $u$ and $v$ are the velocity components of flow particle in $x$ and $y$ directions, $f$ is the Coriolis parameter, $g$ is the acceleration due to gravity, $c_f$ is the friction coefficient.

## III. Boundary-Fitted Grids and Boundary Conditions

Let $x$-axis and $y$-axis of the model domain are considered towards the west and north directions respectively. The eastern moving coastal boundary is situated with the initial position at $x = b_1(y)$ and the western open-sea boundary is at $x = b_2(y)$. The southern and the northern open sea boundaries are at $y = 0$ and $y = L$ respectively. The western, southern and northern open sea boundaries are considered as fixed.

Following [7], the system of gridlines along $x = b_1(y)$ and $x = b_2(y)$ are given by the generalized function,

$$x = \{(k - l)b_1(y) + lb_2(y)\}/k \tag{4}$$

where, $k = M$ is the number of gridlines in $x$-direction and $l$ is an integer such that $0 \le l \le \mathrm{k}$

The system of gridlines along $y = 0$ and $y = L$ are given by the generalized function:

$$y = \{(q - p)0 + pL\}/q \tag{5}$$

where, $q=N$ is the number of gridlines in $y$-direction and $p$ is an integer such that $0 \le \mathrm{p} \le \mathrm{q}$.

The coastal boundary may be of two types: the coastline consists of a vertical side wall or the shoreline moves with the same velocity as that of the approaching water. Following [7], in case of fixed coastal boundary the condition is:

$$u - v\frac{\partial b_1}{\partial y} = 0 \text{ along } x = b_1(y, 0) \tag{6}$$

and in case of moving coastal boundary the condition is:

$$u - \frac{\partial b_1}{\partial t} - v\frac{\partial b_1}{\partial y} = 0 \text{ along } x = b_1(y, t) \tag{7}$$

Following [12], boundary conditions along the open boundaries are:

$$v + (g/h)^{1/2}\zeta = 0 \text{ along } y = 0 \tag{8}$$

$$v-(g/h)^{1/2}\zeta=0 \text{ along } y=L \tag{9}$$

$$u-v\frac{\partial b_2}{\partial y}-\left(\frac{g}{h}\right)^{\frac{1}{2}}\varsigma=0 \text{ along } x=b_2(y) \tag{10}$$

## IV. Transformed Shallow Water Equations and Boundary Conditions

Similar to [12], [13], to facilitate the numerical treatment of the bending coastal boundary, the following coordinate transformation is introduced taking $\eta,\gamma,y,t$ as the new independent variables:

$$\eta=\frac{x-b_1(y)}{b(y)},\quad \lambda=\frac{y}{L},\quad b(y,t)=b_2(y)-b_1(y,t) \tag{11}$$

This mapping transforms the analysis area enclosed by $x=b_1(y), x=b_2(y), y=0$ and $y=L$ into a rectangular domain given by $0\le\eta\le 1,\quad 0\le\lambda\le 1$ .

Using the transformations (11) and (1)-(3) transform to:

$$\frac{\partial(bL\zeta)}{\partial t}+\frac{\partial\tilde{U}}{\partial\eta}+\frac{\partial\tilde{V}}{\partial\lambda}=0 \tag{12}$$

$$\frac{\partial\tilde{u}}{\partial t}+\frac{\partial(U\tilde{u})}{\partial\eta}+\frac{\partial(V\tilde{u})}{\partial\lambda}-f\tilde{v}=-gL(\zeta+h)\frac{\partial\zeta}{\partial\eta}-\frac{C_f\tilde{u}\left(u^2+v^2\right)^{1/2}}{\zeta+h} \tag{13}$$

$$\frac{\partial\tilde{v}}{\partial t}+\frac{\partial(U\tilde{v})}{\partial\eta}+\frac{\partial(V\tilde{v})}{\partial\lambda}+f\tilde{u}=-g(\zeta+h)\left[b\frac{\partial\zeta}{\partial\lambda}-L\left(\frac{db_1}{dy}+\eta\frac{db}{dy}\right)\frac{\partial\zeta}{\partial\eta}\right]-\frac{C_f\tilde{v}\left(u^2+v^2\right)^{1/2}}{\zeta+h} \tag{14}$$

where,

$$U=\frac{1}{b}\left[u-\left(\frac{db_1}{dy}+\eta\frac{db}{dy}\right)v\right],\quad V=\frac{v}{L},\quad (\tilde{u},\tilde{v},\tilde{U},\tilde{V})=bL(\zeta+h)(u,v,U,V)$$

and the boundary conditions are,

$$U=0 \text{ at } \eta=0 \tag{15}$$

$$bU-(g/h)^{1/2}\zeta=0 \text{ at } \eta=1 \tag{16}$$

$$VL+(g/h)^{1/2}\zeta=0 \text{ at } \lambda=0 \tag{17}$$

$$VL-(g/h)^{1/2}\zeta=0 \text{ at } \lambda=1 \tag{18}$$

At each boundary of an island, the normal component of the velocity vanishes. Thus, the boundary conditions of an island are given by:

$$U=0 \text{ at } \eta=l_1/k \text{ and } \eta=l_2/k \tag{19}$$

$$V=0 \text{ at } \lambda=p_1/q \text{ and } \lambda=p_2/q \tag{20}$$

## V. Moving Boundary Technique

In carrying out numerical computations, a computational domain is divided into finite difference grids. Initially, the free surface displacement is zero everywhere, as are the volume fluxes. When a grid point is on dry land, the water depth $h$ takes a negative value and gives the elevation of the land measured from the initial still water level. In general, the moving boundary technique approximates a real topography by a series of small steps with a narrow width. The water depth $h$ is positive when the elevation of bottom is under the still water level, whereas the water depth is negative for an opposite situation. If the total water depth $H$ at a grid point is positive, then the grid point is wet or submerged. On the other hand, a cell is dry or exposed if $H$ is zero. Thus, for the dry area, the free surface displacement $\varsigma$ should be set as $-h$ to give a zero total depth for an exposed area. When tsunami recede, a thin film of water is left on the exposed bottom due to excessively high bottom friction after main water body is removed. Since the location of a boundary cannot be definitely identified in this case, it is necessary to replace $\varsigma$ by $-h$ for this area where the total water depth $H$ is less than a prescribed minimum depth. In case of inland intrusion of water, the continuously deforming position of the coastline is ensured by kinematical boundary condition. A further requirement is that the depth of water be zero at the coastline. Thus, following [14], at $x=b_1(y,t)$ or $\eta=0$

$$\varsigma(\eta=0,y,t)+h(x=b_1(y,t))=0 \tag{21}$$

Depending on whether $b_1(y,t)>b_1(y,0)$ or $b_1(y,t)<b_1(y,0)$, interpolation or use new inland orographical data is used to fix the value of $h(x=b_1(y,t)y)$. This may be achieved by differentiating (21) with respect to t to yield:

$$\frac{\partial\zeta}{\partial t}(\eta=0,y,t)+S\frac{\partial b_1}{\partial t}=0 \tag{22}$$

where;

$$S=\left(\frac{\partial h}{\partial x}\right)_{x=b_1(y,t)} \tag{23}$$

$S$ is the onshore slope of the coastal belt.

Equation (22) gives the value of $b_1(y,t)$ at any time $t$. For a constant value of $S$, by integrating (22) we get,

$$b_1(y,t)=b_1(y,0)-\frac{1}{S}\varsigma(\eta=0,y,t)=0 \tag{24}$$

From (24), it is evident that, if $\varsigma(\eta=0,y,t)<0,$, the water surface at the coastline is depressed and so the coastline will

recede from its initial position. If $\varsigma(\eta = 0, y, t) > 0,$ water surface at the coastline rises above its equilibrium level and so there is corresponding inland intrusion of water. The inland intrusion of water may be determined by:

$$\mu(y,t) = b_1(y,t) - b_1(y,0) \tag{25}$$

## VI. Numerical Discretisation in Transformed Domain Boundary-Fitted Grids and Boundary Conditions

In the physical domain, the curvilinear grid system and in the transformed domain, the corresponding rectangular grid system is generated. Discrete coordinate points in the transformed domain at the respective grid widths $\Delta\chi, \Delta\lambda$ and we define the grid points $(\Delta\chi, \Delta\lambda)$ in the domain by:

$$\chi_i = (i-1)\Delta\chi\ ,\ i = 1,2,3,....,m \tag{26}$$

$$\lambda_i = (j-1)\Delta\lambda\ ,\ j = 1,2,3,....,n \tag{27}$$

The sequence of discrete times using the time step $\Delta t$ is:

$$t_k = k\ \Delta t\ ,\ k = 1,2,3,.... \tag{28}$$

A staggered grid system, similar to Arakawa C system, is used in the transformed domain where there are three distinct types of computational points. These three types of points are defined as follows: For every discrete grid point $(\chi_i, \lambda_j)$, if $i$ is even and $j$ is odd, the point is a $\varsigma$ -point at which $\varsigma$ is computed. If $i$ is odd and $j$ is odd, the point is a $u$ -point at which $u$ is computed. If $i$ is even and $j$ is even, the point is a $v$ -point at which $v$ is computed. In a staggered grid system, since every dependent variable is computed at any one of these three types of points rather than at every point, the CPU time is reduced. Moreover, a staggered grid system is favorable in filtering out sub-grid scale oscillations.

The transformed shallow water (12)-(14) together with the boundary conditions (16)-(18) are discretized by finite difference (Forward Time Centred Space) and are solved by a conditionally stable semi-implicit method. The χ-axis is directed towards west at an angle 15° (anticlockwise) with the latitude line and the λ -axis is directed towards north inclined at an angle 15° (anticlockwise) with the longitude line. The number of grids in χ and λ - directions are respectively $m$ =230 and $n$ = 319 and the grid size is chosen to be equal to 4 km.

The model area (Fig. 1) includes the source region of Indonesian tsunami 2004. The time step of computation is determined to satisfy the stability condition (Courant condition). It is set to 10 s in this computation. Following [6], the value of the friction coefficient C$f$ taken as 0.0033 throughout the model area. The depth data for the model area are collected from the Admiralty bathymetric charts. The depth at the entire rest grid points of the mesh are computed by some averaging process. The bathymetry of the model domain is shown in Fig. 2.

## VII. Initial Condition (Tsunami Source Generation)

The generation of an earthquake tsunami source depends essentially on the pattern and dynamics of motions in the earthquake source zone and on the initial seafloor movements. The generation mechanism of the 2004 Indonesian tsunami was mainly a static sea floor uplift caused by an abrupt slip at the India/Burma plate interface. A detailed description of the estimation of the extent of the earthquake rapture as well as the maximum uplift and subsidence of the seabed is given in [6] and this estimation is based on [15]. The deformation contour reveal that the estimated uplift and subsidence zone is between 92°E to 97°E and 2°N to 10°N with a maximum uplift of 507 cm at the west and maximum subsidence of 474 cm at the east. The uplift to subsidence is approximately from west to east relative to the west coasts of the Malaysian Peninsula and Thailand. The major force of tsunamis is the vertical displacement of the seafloor. For computational purposes tsunami models are often initialized by a sea-surface displacement. We can assume that the initial value of the sea surface displacement that starts a tsunami is the same as the vertical displacement of the sea floor, due to incompressibility of the ocean water [16]. Following [6], the disturbance in the form of rise and fall of sea surface is assigned as the initial condition in both the models with a maximum rise of 5 m to maximum fall of 4.75 m. Ammon et al. [17] reported the rupture zone between 92° E to 97°E and 2°N to 13°N. Tanioka et al. [18] estimated the rupture zone between 92° E to 97°E and 2°N to 13.5°N. Based on the information available in [6], [17] and [18], we consider the source, extended along the fault line between 92° E to 97°E and 2°N to 10°N for our model. In all other regions, the initial sea surface elevations are taken as zero. Also, the initial $x$ and $y$ components of velocity are taken as zero throughout the model area.

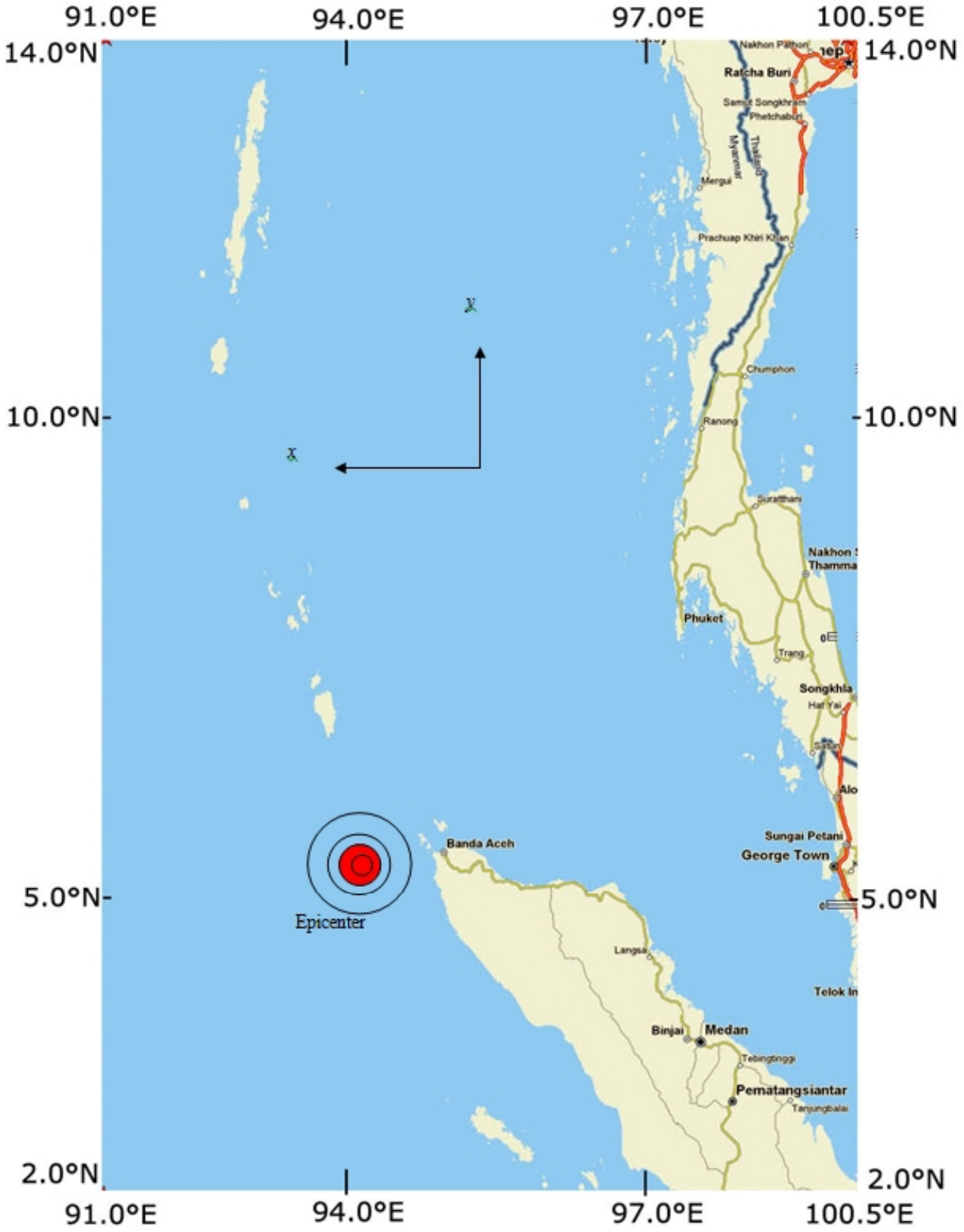


Fig. 1 Model Domain including the coastal geometry and the epicenter of the 2004 earthquake

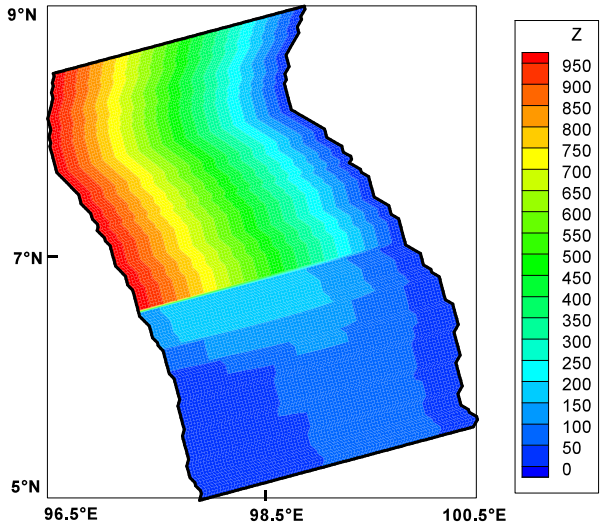


Fig. 2 Bathymetry used in the numerical simulation (depth unit in meter)

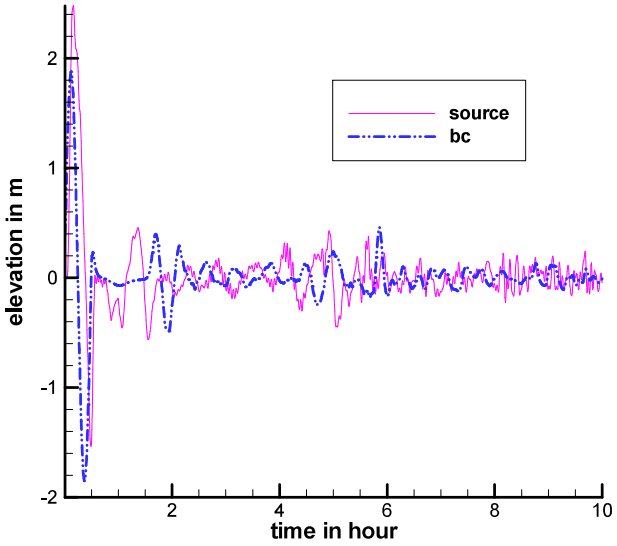


Fig. 3 Time series of sea surface fluctuation at the western open boundary

## VIII. Open Boundary Condition for Far Field Tsunami Computation

The time series of the sea surface fluctuation and amplitude of the source of Indonesian tsunami 2004 along the western open boundary of the model has been computed. To simulate the far field tsunami or to investigate the effect of a far field tsunami it is considered that the tsunami source is located far away from the model domain. The amplitudes of tsunami wave along the western open boundary as the response of the source has been computed to estimate the amplitude of the boundary condition by which far field tsunami will be computed in absence of the source. Similar [8], for generating tsunami response in a limited area model through a boundary, an open boundary condition is formulated by associating a sinusoidal term, containing amplitude, period and phase, with the radiation type of boundary condition [6] and this is described as:

$$u-(g/h)^{1/2}\zeta = \quad \text{at } x=b_2(y) \qquad (29)$$
$$-2(g/h)^{1/2}e^{(-st)}a\sin(2\pi t/T+\varphi)$$

where, $a$ is the amplitude, $T$ is the period, $\varphi$ is the phase of the wave. But for tsunami propagation the time series is oscillatory with damping amplitude. On the basis of time series data and amplitude presented in Fig. 3, the open boundary condition similar to [5] that represents the effect of far field tsunami for the boundary fitted curvilinear model is

$$bU-(g/h)^{1/2}\zeta = \quad \text{at } x=b_2(y) \qquad (30)$$
$$-2(g/h)^{1/2}e^{(-st)}a\sin(2\pi t/T+\varphi)$$

where, $s$ is the scale factor used for damping the amplitude of the wave with respect to time, $s=0$ for $t\le T$ and $s>0$ for $t>T$. Using these conditions, we are allowing one wave, with full amplitude, to enter into the domain through the open boundary before damping of the amplitude begins.

The assigned amplitudes ($a$) in (30) are adjusted so that the response of the boundary condition in model domain is similar to that associated with the source of Indonesian tsunami 2004. By trial and error method, the values of phase ($\phi$), period ($T$) and the scale factor in (30) have also been adjusted and these are $\varphi=0, T=0.5$ hr and $s=0.01$. Fig. 3 shows the time series of sea surface fluctuation at (230, 155) the grid point at the western open boundary due to the source of Indonesian tsunami 2004 and the boundary condition. Both the time series are found to be almost identical, which means that the boundary condition is capable of generating time series which is similar to that generated by the source.

## IX. Combined Effect of Open Boundary Condition and Moving Boundary Condition

We have explained here in detail the inland inundation, the tsunami propagation and run-up along the western coastal belt of Peninsular Malaysia and southern Thailand in order to present the effect of moving boundary condition in far field tsunami computation in a limited area model domain. In addition, we have established a good relationship between inundation and water level. We have also discussed the comparison of maximum water level along the coast obtained from the model of moving boundary and the model of fixed coastal boundary.

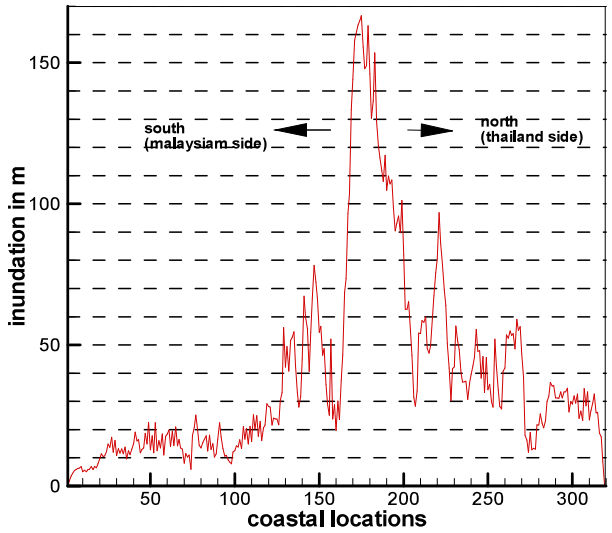


Fig. 4 Maximum inland inundation along the west coast of Peninsular Malaysia and Thailand for 8 degree inclination

*A. Inland Inundation Level*

In Fig. 4, we have shown the maximum inland inundation along the west coast of Thailand and Peninsular Malaysia for an inclination of 8 degree. The maximum inland disturbance along west coast of Peninsular Malaysia is about 30 m while along the Thailand coast it is about 170 m. Fig. 5 shows that as the on-shore inclination increases from 8 degree to 12 degree, the level of inundation decreases to nearly 20 m and 115 m for the coastal belts of Malaysia and Thailand respectively. If the slopes of Malaysia and Thailand coast vary from 8 degree to 12 degree, the inundations then vary from nearly 40 m to 200 m respectively as shown in Fig. 6. Therefore, we may conclude that the tsunami inundation is controlled by the configuration of the beach. According to the report of eyewitnesses from a post tsunami field survey along the coastal belt of southern Thailand conducted by [19], the tsunami inundation in the Patong beach of Thailand varied from 150 m to at least 750 m while in Maya Bay it varied from 200 m to 300 m. But we have not found here any information regarding the extent of inundation along the Malaysia coast. Moreover, the actual onshore slope of the coastal belt is not considered in the model computations. However, our computed result shows good agreement with the field survey report of [19].

*B. Relationship between Inundation and Water Level*

Fig. 7 depicts the computed time series of water level at a coastal location of Thailand about 140 km north of Phuket due to the initial tsunami generated at Sumatra on 26 December 2004. At the south coast of Phuket the time series begins with recession that reaches a depression of –2.5 m before rising up; then the water level gradually increases to reach a maximum level of 11.6 m. The water level then oscillates continuously for several hours with low amplitude. Besides, Fig. 8 shows the computed inundation and recession for the same coastal location due to 8 degree inclination associated with the tsunami wave. For 8 degree inclination the inland inundation/recession curve is consistent with the water level fluctuation with a maximum inundation of 82 m and maximum recession of -35 m. Since the slope is considered as constant, the curve of inundation/recession should be consistent with that of sea surface oscillation. As the on-shore slope increases the computed inundation/recession remains qualitatively the same but both inundation and recession amplitudes gradually decrease.

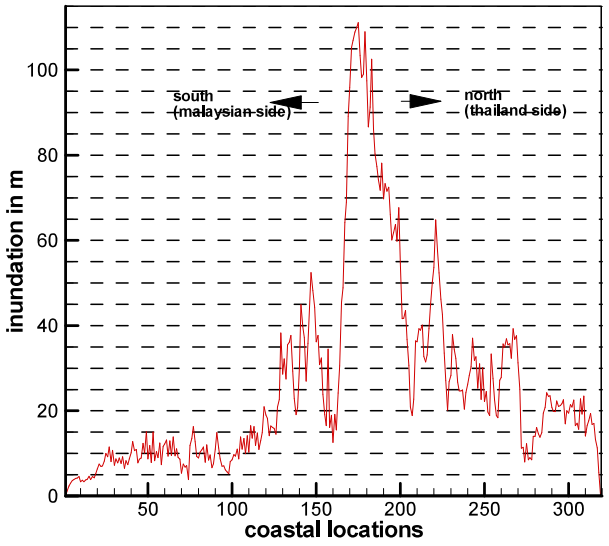


Fig. 5 Maximum inland inundation along the west coast of Peninsular Malaysia and Thailand for 12 degree inclination

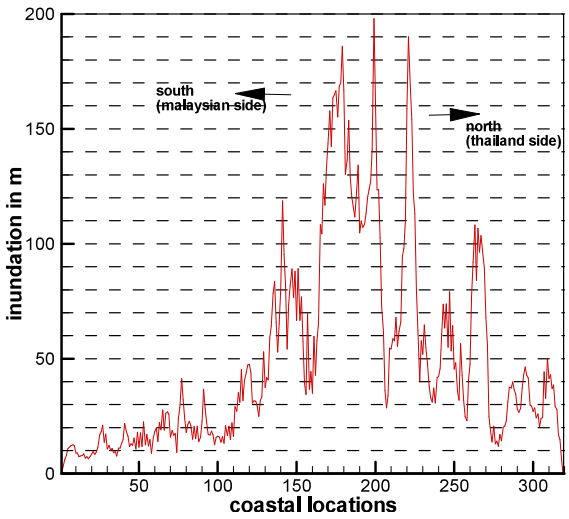


Fig. 6 Maximum inland inundation along the west coast of Peninsular Malaysia and Thailand for variable degree inclination

*C. Correlations between the Maximum Water Levels Due to Moving and Fixed Coastal Boundary*

Fig. 9 shows the comparison of the elevation of water level at a particular coastal location near the south of Phuket island and Thailand island due to the moving and fixed coastal boundary. In this figure, we have observed that the maximum

water level is about 10.75 m along the coast due to moving boundary and the peak surge is about 12 m due to fixed coastal boundary. The surge height along the fixed boundary is significantly higher than that of the moving boundary. This is maybe due to the unrealistic piling up of water at the vertical side wall boundary. On the other hand, this piling up does not occur since the water is allowed to flow inland freely. Thus reducing the maximum sea surface elevation at the initial position of the coast line causes the inundation.

## X. Conclusion

A moving boundary condition and an open boundary condition are simultaneously used to simulate the extent of inland inundation due to far field tsunami in a limited area model domain. The moving boundary technique is used to tract movements of shore as tsunamis rises and recedes. The inundation along the coastal belt of the west coast of Peninsular Malaysia and southern Thailand due to the 24 December 2004 Indonesian tsunami is found to decrease with the increase of the slope of the beach and the inundation is controlled by the configuration of the beach. An investigation is carried out to test the relation between the maximum water level and inundation/recession along the coast and it seems that the inundation/recession and water level are directly proportional to each other. A comparison of maximum water levels due to moving boundary and fixed coastal boundary was also carried out. The water elevation due to fixed boundary is considerably higher than that of moving boundary. The proposed numerical model successfully simulates the long wave inundation along the coast due to far field tsunami specially when the coast is far from the tsunami source.

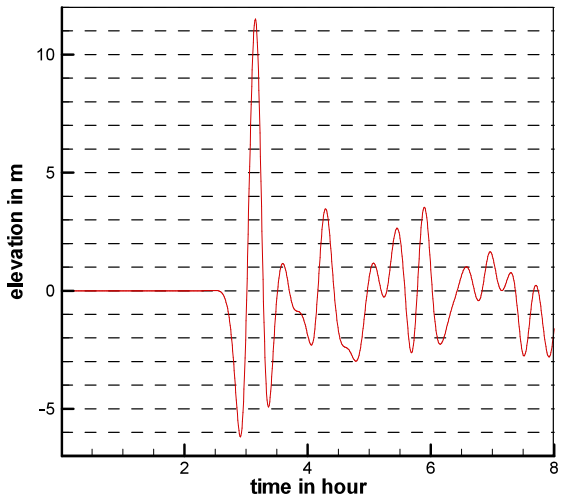


Fig. 7 Time series of water elevation along a particular coastal location of Southern Thailand

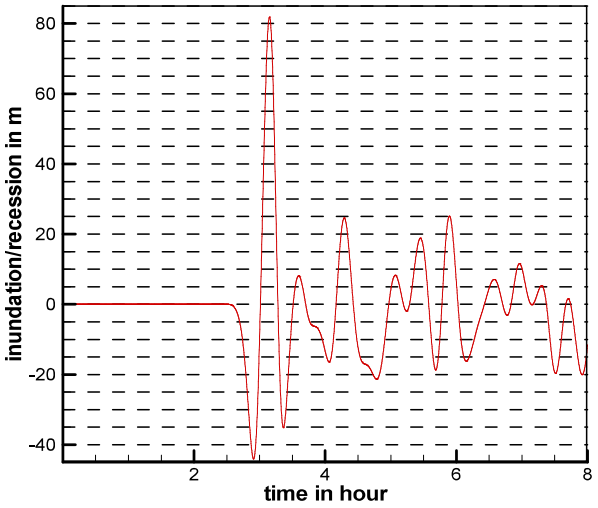


Fig. 8 Comparison of water elevation and inundation along a particular coastal location of southern Thailand

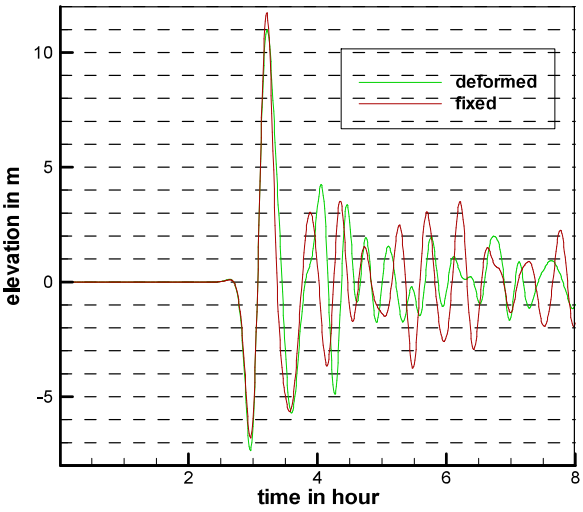


Fig. 9 Comparison of water elevation along a particular position of the coast due to fixed boundary and deformed/moving coastal boundary

## References

[1] Yoon, S. B., "Propagation of tsunamis over slowly varying topography", Journal of Geophysical Research, 107 (C10), 4(1) – 4(11), 2002.

[2] Karim, M. F., Roy, G. D., Ismail, A. I. M., and Meah, M. A., "A linear Cartesian coordinate shallow water model for tsunami computation along the west coast of Thailand and Malaysia", Int. J. of Ecology & Development 4(S06): 1 – 14, 2006.

[3] Karim, M. F., Ismail, A. I. M., and Meah, M.A., "Numerical Simulation of Indonesian Tsunami 2004 at Penang Island in Peninsular Malaysia using a Nested Grid Model", International Journal of Mathematical Models and Methods in Applied Sciences, vol 3, Issue 1, 1-8, 2009(a).

[4] Karim, M. F., Roy, G. D., Ismail, A. I. M. and Meah, M.A., "Numerical Simulation of Indonesian Tsunami 2004 along Southern Thailand: A Nested Grid Model", International Journal of Mathematical, Physical and Engineering Sciences, vol 3 (1),8-14, 2009(b).

[5] Roy, G. D., Karim, M. F. & Ismail, A. M., "Numerical Computation of Some Aspects of 26 December 2004 Tsunami along the West Coast of Thailand and Peninsular Malaysia Using a Cartesian Coordinate Shallow Water Model", Far East J. Appl. Math., 25(1), 57-71, 2006.

[6] Kowalik, Z., Knight, W. and Whitmore, P. M.," Numerical Modeling of the Tsunami: Indonesian Tsunami of 26 December 2004", Journal of Science of Tsunami Hazards, 23(1), 40 – 56, 2005.
[7] Karim, M. F., Esa, A. I., "A Boundary Fitted Nested Grid Model for Modelling Tsunami Propagation of 2004 Indonesian Tsunami along Southern Thailand", International Journal of Environmental, Chemical, Ecological and Geophysical Engineering, vol 9(8) 891 – 898, 2015.
[8] Karim, M. F., Roy, G. D., and Ismail, A. I. M., "A Study of Open Boundary Conditions for Far Field Tsunami Computation", WSEAS Transactions on Environment and Development, vol 4 (4), 334–349, 2008.
[9] Cho, Y.S. and Kim, J.M., "Moving Boundary Treatment in Run-up process of Tsunami", Journal of Coastal Research, SI 56, Proceedings of the 10th International Coastal Symposium, Lisbon, Portugal, 482-486, 2009.
[10] Inan, A., and Balas, L. A., "Moving Boundary Wave Run-Up Model" In Y. Shi, Albada, G.D.v., Dongarra, J., & Sloot, P.M.A. (Ed.), Berlin Heidelberg: Springer, Computational Science – ICCS, 38-45, 2007.
[11] Roy, G.D., Karim, M.F., and Ismail, A.I.M., "A 1-D Shallow Water Model for Computing Inland Inundation due to Long Waves Using a Moving Boundary", Far East Journal of Applied Mathematics 28(3), 395, 395-408, 2007.
[12] Karim, M.F., Meah, M.A. and Ismail, A.I.M., "A Shallow Water Model for Computing Inland Inundation due to Indonesian Tsunami 2004 using a Moving Coastal Boundary", World Academy of Science, Engineering and Technology, vol 72, 1777 – 1782, 2012.
[13] Meah, M.A., Ismail, A.I.M., Karim, M.F., and Islam, M.S., "Simulation of the Effect of Far Field Tsunami Through an Open Boundary Condition in a Boundary-Fitted Curvilinear Grid System" Journal of Science of Tsunami Hazards. Vol. 31(1), 1 – 18, 2012.
[14] Karim, M. F., Roy, G.D., Ismail, A. I. M., and Meah, M.A., "A Shallow Water Model for Computing Tsunami along the West Coast of Peninsular Malaysia and Thailand Using Boundary- Fitted Curvilinear Grids", Science of Tsunami Hazards, 26 (1), 21 – 41, 2007.
[15] Okada, Y., "Surface Deformation due to Shear and Tensile Faults in a Half Space", Bull, Seism. Soc. Am., 75, 1135 – 1154, 1985.
[16] Arreaga-Vargas, P., Ortiz, M., and Farreras, S.F., "Mapping the Possible Tsunami Hazard as the First Step Towards a Tsunami Resistant Community in Esmeraldas, Ecuador", In K. Satake (Ed.), Tsunamis: Case Studies and Recent Developments, Netherlands: Springer, 203 – 215, 2005.
[17] Ammon, C. J., Ji, C., Thio, H.-K.., Robinson, D., Ni, S., Hjorleifsdottir, V., Kanamori, H., Lay, T., Das, S., Helmberger, D., Ichinose, G., Polet, J., and Wald, D., "Rupture Process of the 2004 Sumatra-Andaman Earthquake", Science, 308, 1133 – 1139, 2005.
[18] Tanioka, Y., Yudhicara, Kususose, T., Kathiroli, S., Nishimura, Y., Iwasaki, S., and Satake, K.., "Rapture process of 2004 great Sumatra-Andaman earthquake estimated from tsunami waveforms, Earth Planets Space, 58, 203 – 209, 2006.
[19] Papadopoulos, G. A., Caputo, R., McAdoo, B., Pavlides, S., Karastathis, V., Fokaefs, A., Orfanogiannaki, K. and Valkaniotis, S., "The large tsunami of 26 December 2004: Field observations and eyewitnesses accounts from Sri Lanka", Maldives Is. and Thailand, Earth Planets Space, 58, 233 – 241, 2006.